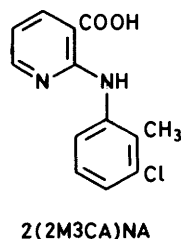


Infrared Spectral and X-Ray Studies of Polymorphic Forms of 2-(2-Methyl-3-chloroanilino)nicotinic Acid

By Mamoru Takasuka,* Hiroshi Nakai, and Motoo Shiro, Shionogi Research Laboratories, Shionogi and Co. Ltd., Fukushima-ku, Osaka 553, Japan

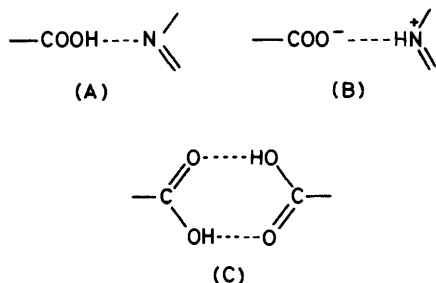
The polymorphic forms of 2-(2-methyl-3-chloroanilino)nicotinic acid, $C_{13}H_{11}ClO_2N_2$, were classified as (I)–(IV) by their i.r. and u.v. spectra, thermograms, and X-ray powder diffraction patterns. Form (I) is monoclinic, space group $P2_1/c$, $a = 7.625(1)$, $b = 14.201(1)$, $c = 11.672(1)$ Å, $\beta = 101.65(1)^\circ$, and $Z = 4$. Form (II) is orthorhombic, space group $Pca2_1$, $a = 23.597(6)$, $b = 4.042(1)$, $c = 12.127(3)$ Å, and $Z = 4$. Form (III) is triclinic, space group $P\bar{1}$, $a = 13.810(1)$, $b = 3.858(1)$, $c = 10.984(2)$ Å, $\alpha = 94.98(1)$, $\beta = 94.42(1)$, $\gamma = 95.57(1)^\circ$, and $Z = 2$. Form (IV) is triclinic, space group $P\bar{1}$, $a = 7.670(1)$, $b = 7.254(1)$, $c = 10.882(1)$ Å, $\alpha = 100.66(1)$, $\beta = 102.02(1)$, $\gamma = 86.97(1)^\circ$, and $Z = 2$. Assignments of the i.r. vibration bands to the intra- and inter-molecular hydrogen bonds have been performed taking into consideration the deuterium isotopic effects, the spectral changes observed at low temperature and the spectra of related compounds. Three types of intermolecular hydrogen bonds (A)–(C) were respectively allocated to forms (I), (II), and (III) and (IV). The intramolecular hydrogen bonds found in all forms were identified as $>NH \cdots O$. The crystal structures were determined by X-ray analysis. The results confirmed the hydrogen bonds indicated by the i.r. spectral study. Relationships were established between the AH stretching frequencies and the $A \cdots B$ distances for the intra- and inter-molecular $AH \cdots B$ hydrogen bonds detected in all the forms. Shifts of the longest wavelength band in the u.v. spectra were correlated with the dihedral angles between the pyridine and benzene rings.

CRYSTALS of 2-(2-methyl-3-chloroanilino)nicotinic acid, 2(2M3CA)NA, are obtained in four polymorphic forms referred to as forms (I)–(IV). Different types of intermolecular hydrogen bonds, detected in the crystals of



nicotinic acid (A),¹ cinchoneric acid [a zwitterion form: (B)],² and benzoic acid (C)³ were expected to exist. An i.r. spectral study was used to identify the hydrogen bonds in the relevant forms by comparison with the spectra of crystals of the related compounds described above. X-Ray analyses were undertaken to confirm the hydrogen bonding systems and to identify the detailed crystal and molecular structures.

Correlations between the AH stretching frequencies and the distances $A \cdots B$ have been reported for intermolecular hydrogen bonds $AH \cdots B$ in crystals,^{4–7} but few for intramolecular hydrogen bonds. These correl-



ations for the hydrogen bonds in the four forms are discussed here.

The correlation between the u.v. spectra and the twist angles of the benzene ring is also considered.

EXPERIMENTAL

Crystals in forms (I)–(IV) were respectively obtained from ethyl acetate, methanol, ethanol, and acetone solutions. The deuteriated molecule, $[^2H_2]2(2M3CA)NA$, in which the OH and NH groups were substituted with deuterium atoms, could be crystallized in forms (I), (III), and (IV) from dry ethyl acetate, methan[2H]ol, and dry acetone solutions, respectively, but not in form (II) from all the recrystallization solvents examined. The polymorphic forms of $[^2H_2]2(2M3CA)NA$ indicated by the corresponding number with the suffix D were identified from the X-ray powder diffraction patterns.

I.r. Spectroscopy.—I.r. spectra of 2(2M3CA)NA and $[^2H_2]2(2M3CA)NA$ in $CHCl_3$ solutions and their crystals in the respective polymorphic forms were recorded on a JASCO DS-403G grating spectrometer. Spectra of the following compounds were taken for reference: nicotinic acid (NA), nicotinic [2H]acid ($[^2H]NA$), sodium nicotinate (NANa), benzoic acid (BA), benzoic [2H]acid ($[^2H]BA$), sodium benzoate (ABNa), salicylic acid (SA), sodium salicylate (SANA), sodium [$O-^2H$]salicylate, *N*-phenylanthranilic acid (NPAA), [$O,N-^2H_2$]-*N*-phenylanthranilic acid ($[^2H_2]NPAA$), sodium *N*-phenylanthranilate (NPAANA), sodium [$N-^2H$]-*N*-phenylanthranilate, diphenylamine (DPA), and [$N-^2H$]diphenylamine. The deuteriated molecules were obtained by evaporation of acetone- D_2O or ethan[2H]ol solution.

U.v. Spectroscopy.—U.v. spectra of 2(2M3CA)NA in $CHCl_3$ solution and those for crystals of forms (I)–(IV) milled in Nujol oil were recorded on a Hitachi EPS-3T spectrophotometer, using a diffuse reflectance accessory for the latter.

Thermoanalysis.—Thermograms were taken on a Rigaku TG-DSC 8085C instrument.

X-Ray Powder Diffraction.—A Nonius Debye-Scherrer camera was employed to obtain the X-ray powder diffraction patterns of all the polymorphic forms studied.

Crystal Structure Analysis.—Crystal data which are not given in the Abstract are listed in Table 1. The centrosymmetric space group *PI* for forms (III) and (IV) was assumed from the statistical distribution of *E* and verified after the crystal structure refinement. Three-dimensional intensity data were collected on a Hilger and Watts Y-290 diffractometer equipped with a scintillation counter and a pulse-height analyser. Integrated intensities were

cycle were sufficiently small compared with σ . The atomic scattering factors were taken from ref. 10.

RESULTS AND DISCUSSION

I.r. Spectral Assignment and Inter- and Intra-molecular Hydrogen Bonds.—The band assignments shown in Table 2 were based on consideration of the deuterium isotopic effects and spectral changes exhibited at low temperature and on comparison with the spectra of the related compounds in crystalline states and CHCl_3

TABLE 1
Crystal data

Form	(I)	(II)	(III)	(IV)
Colour	Colourless	Pale yellow	Yellow	Yellow
$U/\text{\AA}^3$	1 237.8	1 156.6	578.1	581.8
$D_x/\text{g cm}^{-3}$	1.41	1.51	1.51	1.50
$D_m/\text{g cm}^{-3}$	1.40	1.50	1.50	1.49
Crystal size (mm)	$0.3 \times 0.3 \times 0.3$	$0.1 \times 0.1 \times 0.4$	$0.2 \times 0.1 \times 0.3$	$0.3 \times 0.3 \times 0.3$
Linear absorption coefficient μ (Mo- K_α)/ cm^{-1}	3.21	3.44	3.44	3.42
Systematically absent reflections				
0 <i>kl</i>		$l = 2n + 1$		
<i>h</i> 0 <i>l</i>	$l = 2n + 1$	$h = 2n + 1$		
<i>h</i> 00		$(h = 2n + 1)$		
0 <i>h</i> 0	$h = 2n + 1$			
00 <i>l</i>		$(l = 2n + 1)$		
Number of reflections measured ($\theta_{\text{max.}}/^\circ$)	1 416 (21.5)	799 (22.5)	1 506 (22.5)	2 048 (25.0)

measured by the θ - 2θ scan technique using zirconium-filtered Mo- K_α radiation. Each reflection was integrated in 80 steps at intervals of 0.01° . The measurement time was 1 s per step. Backgrounds were counted for 20 s on both sides of each reflection. One standard reflection monitored every 10 reflections showed no significant change in intensity during data collection. All intensities were corrected for Lorentz and polarization factors, but not for absorption effects.

Structure Determination and Refinement.—The structures were solved using the program MULTAN⁸ with local modifications on a FACOM 270-30 computer. A difference electron density map was calculated after block-diagonal least-squares refinement, which revealed the positions of all the hydrogen atoms. Successive refinement of the positional and anisotropic thermal parameters of the non-hydrogen atoms gave the *R* values ($R = \Sigma|\Delta F|/\Sigma|F_o|$) of 0.052 (1 206 reflections) for form (I), 0.065 (619) for form (II), 0.070 (960) for form (III), and 0.048 (1 761) for form (IV).^{*} The standard deviation of each reflection was taken as $\sigma(F_o) = [\sigma_1^2(F_o) + c^2|F_o|^2]^{1/2}$, where $\sigma_1(F_o)$ is the estimated standard deviation due to the counting errors.⁹ Values of c^2 were 0.001 54, 0.000 34, 0.000 81, and 0.001 76 for forms (I)—(IV), respectively. The weighting scheme used was $w = 1/\sigma^2(F_o)$ for $|F_o| \geq n\sigma(F_o)$ and $w = 0$ for $|F_o| < n\sigma(F_o)$ or $|\Delta F| \geq 3\sigma(F_o)$, where n is 1 for forms (I) and (IV) and 2 for forms (II) and (III). The function minimized in the refinement is $\Sigma(w|\Delta F|^2)$. The parameter shifts in the final

solutions. Isotopic frequency ratios are listed in Table 3.

The values of ν_{OH} , δ_{OH} , γ_{OH} , and $\Delta\nu_{\text{C-O}}$ of the carboxy-group in form (I) are similar to those in NA, and those in forms (III) and (IV) to those in BA. They suggest that the intermolecular hydrogen bond in form (I) is of the same type as that in NA (A), and those in forms (III) and (IV) as that in BA (C).

The ν_{NH} band of DPA in dilute CHCl_3 appears at $3\ 431\ \text{cm}^{-1}$ and that of NPAA at $3\ 336\ \text{cm}^{-1}$. The shift of the latter band to the lower wavenumber results from the formation of the intramolecular hydrogen bond $\text{>NH} \cdots \text{O}=\text{C}(\text{OH})^-$. That the wavenumbers of ν_{NH} of 2(2M3CA)-NA in dilute CHCl_3 ($3\ 335\ \text{cm}^{-1}$) and in forms (I)—(IV) are nearly equal to or lower than that of NPAA indicates the existence of such a hydrogen bond in this molecule.

In the spectrum of form II, the bands corresponding to the ν_{OH} , δ_{OH} , and γ_{OH} bands of the other forms do not appear. This suggests that the molecule in the crystal in form (II) has a carboxylate group, and it thus takes a zwitterion form as shown in the chart below.

The ν_{CO} bands (ν_{as} and ν_{s} in Table 2) of the carboxylate group in form (II) were identified by referring to those of NANA. In the spectra of SANA and NPAANA in which the intramolecular hydrogen bonds $-\text{COO}^- \cdots \text{HO}-^{11}$ and $-\text{COO}^- \cdots \text{HN}<$ are respectively formed, the ν_{as} bands shift to higher wavenumbers than that in BANa and the ν_{s} bands to lower wavenumbers. Similar shifts observed between those bands of NANA and form (II) reveal the formation of the intramolecular hydrogen bond $-\text{COO}^- \cdots \text{NH}<$ in form (II). As such a hydrogen bond is assumed to be stronger than the hydrogen bond

* X-Ray powder diffraction data, i.r. spectra, bond lengths and angles, crystal structures, structure amplitudes, and anisotropic thermal parameters of the non-hydrogen atoms for the four polymorphic forms are listed in Supplementary Publication No. SUP 23322 (50 pp.). For details see Notices to Authors No. 7 in *J. Chem. Soc., Perkin Trans. 2*, 1981, Index Issue.

TABLE 2

I.r. spectra data of the polymorphic forms of 2(2M3CA)NA and [$^2\text{H}_2$]2(2M3CA)NA and the related compounds (Nujol and perfluorocarbon mulls)

Compound	ν_{NH}	δ_{NH}	γ_{NH}	Mode a (cm^{-1})	ν_{OH}	δ_{OH}	γ_{OH}	COOH	
	ν_{ND}	δ_{ND}	γ_{ND}		ν_{OD}	δ_{OD}	γ_{OD}	$\nu_{\text{C=O}}$	$\nu_{\text{C-O}}$
NA				{ 2 416 1 900	1 490		1 020	1 702	{ 1 323 1 301
[^2H]NA				~1 890	1 075		~750	1 696	1 343
BA				{ ~2 940 ~2 600	1 424		935	1 689	{ 1 326 1 292
[^2H]BA				{ 2 231 2 070	1 043			1 683	1 367
NPAA	{ 3 340 3 329	1 590	~500	{ ~3 000 ~2 700	1 436		~900	1 660	1 325
[$^2\text{H}_2$]NPAA	{ 2 481 2 466	1 389	392	{ 2 241 2 060	1 036			1 650	
Form									
(I)	3 223	1 595	607	{ 2 458 1 862	1 508		976	1 680	1 298
(I) _D	2 402	1 387	445	{ ~1 956	1 098		~725	1 670	1 335
(III)	3 327	1 609	647	{ ~2 940 ~2 630	1 427		889	1 668	1 298
(III) _D	2 454	1 395	474	{ 2 240 2 060	1 028		635	1 659	1 343
(IV)	3 306	1 619		{ ~3 050 ~2 700	1 425		850	1 679	1 289
(IV) _D	2 435	1 394		{ 2 257 2 065	1 030		608	1 664	1 343
(II)	3 008			$\nu_{\text{N}^+\text{H}}$ 2 712				$\nu_{\text{as}}(\text{COO}^-)$ 1 646	$\nu_{\text{s}}(\text{COO}^-)$ 1 378
NANa								1 613	1 412
BANa								1 552	{ 1 399 1 385
SANa								1 597	1 377
NPAANa								1 612	1 387

a The ν , δ , and γ indicate stretching, in-plane bending, and out-of-plane bending vibrations, respectively (ν_{as} asymmetric $\nu_{\text{C-O}}$ band and ν_{s} symmetric one).

$>\text{NH} \cdots \text{O}=\text{C}(\text{OH})^-$, the ν_{NH} band of form (II) appears at a lower wavenumber than do those of the other forms.

The band at 2 712 cm^{-1} in the spectrum of form (II) was attributed to $\nu_{\text{N}^+\text{H}}$ of the protonated pyridine ring.

The carboxy-group, N(7), and C(8) of the molecule in each form almost lie on the plane of the pyridine ring. The substituted benzene ring is twisted from the plane about the N(7)-C(8) bond. The twist angles are respectively 70.8(1), 40.2(4), 21.2(2), and 1.7(1) $^\circ$ for forms

TABLE 3

Deuterium isotopic effects in i.r. spectra of NA, BA, NPAA, and forms (I)—(IV) of 2(2M3CA)NA

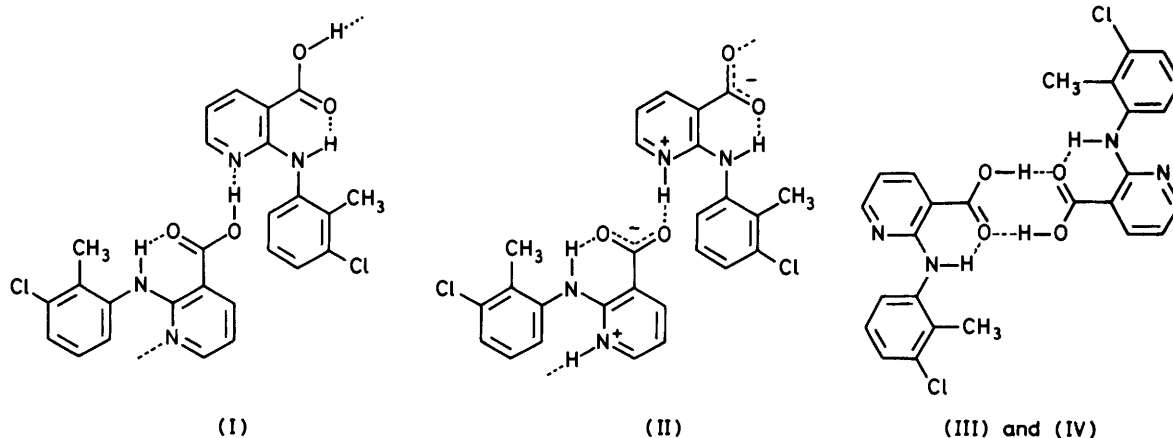
Compound	$\nu_{\text{NH}}/\nu_{\text{ND}}$	$\delta_{\text{NH}}/\delta_{\text{ND}}$	$\gamma_{\text{NH}}/\gamma_{\text{ND}}$	$\nu_{\text{OH}}/\nu_{\text{OD}}$	$\delta_{\text{OH}}/\delta_{\text{OD}}$	$\gamma_{\text{OH}}/\gamma_{\text{OD}}$	$\Delta\nu_{\text{C-O}}^a$
NA				1.28	1.39		31
BA				1.32	1.37	1.35	58
				1.25			
NPAA	1.35	1.14	1.28	1.34	1.39		
	1.35			1.31			
(I)	1.36	1.15	1.36	1.31	1.38	1.35	37
(III)	1.36	1.15	1.36	1.31	1.38	1.40	45
				1.28			
(IV)	1.36	1.16		1.35	1.39	1.40	54
				1.31			

$^a \Delta\nu_{\text{C-O}} = \nu_{\text{C-O}}^{\text{D}} - \nu_{\text{C-O}}^{\text{H}}$.

It was supposed that the intermolecular hydrogen bond $-\text{COO}^- \cdots \text{HN}^+$ might be present in form (II) as in the crystal of cinchomeric acid.²

Crystal and Molecular Structures.—The atom numbering scheme is shown in Figure 1. Final positional and equivalent isotropic thermal parameters of the non-hydrogen atoms are given in Table 4. The structure of form (II) could be determined with less accuracy than those of the other forms because of the smallness of the crystal used.

(I)—(IV). As the twist angle increases, the π -conjugation throughout the whole molecule *via* the lone pair orbital of N(7) decreases; the lone pair orbital is a *p*-type orbital because the sums of angles around N(7) in all the forms were found to be 360 $^\circ$. Hence, the bond length N(7)-C(8) [1.435(5), 1.40(1), 1.402(7), and 1.402(3) Å for forms (I)—(IV), respectively], gradually losing its partial double bond character with increasing twist angle, is most lengthened in form (I). For the bonds C(2)-N(7), the bond lengths in all the forms are so irregular that the influence of the twist angle on them cannot be confirmed.



The bond angles of C(2)-N(7)-C(8), N(7)-C(8)-C(9), and N(7)-C(8)-C(13) in forms (II)—(IV) deviated from the corresponding values in form (I) to elongate the interatomic distances N(1) ··· H[C(13)] to 2.7 Å in form (II) and to 2.3 Å in forms (III) and (IV).

b and *c* axes, respectively. The hydrogen bond distances of O(16) ··· N(1) are 2.710(4) Å for form (I) and 2.75(1) Å for form (II). As seen in Figure 2, the C(6)-H bonds closely approach the O(17) atoms. The interatomic distances of C(6) ··· O(17) and H[C(6)] ··· O(17) are respectively 3.091(5) and 2.30(4) Å for form (I), and 3.14(1) and 2.3(1) Å for form (II). The formation of the

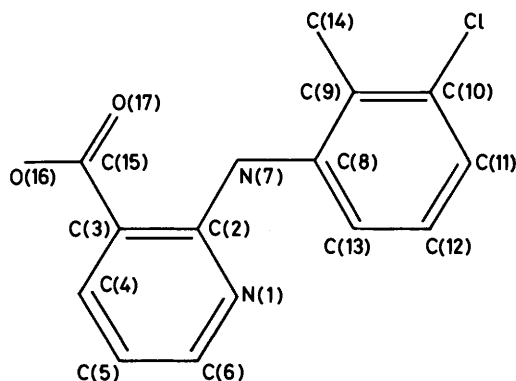


FIGURE 1 Atom-numbering scheme

The difference electron density map of form (II) revealed that the carboxy-group donates its proton to the pyridine nitrogen atom with which it forms the intermolecular hydrogen bond $\text{-COO}^- \cdots \text{HN}^+$. The molecule, therefore, adopts a zwitterion form as shown. Protonation at N(1) in the zwitterion is also confirmed by the enlargement to 123(1)° of the C(2)-N(1)-C(6) bond angle, of which the mean value in forms (I), (III), and (IV) is 118.4(2)°, as in the case of the zwitterion of cinchomeronic acid.² That the bond lengths of C(15)-O(16) [1.22(1) Å] and C(15)-O(17) [1.23(1) Å] in form (II) are almost the same indicates the ionization of the carboxy-group.

The intramolecular hydrogen bonds N(7)-H ··· O(17) are found in all the forms. The distances N(7) ··· O(17) are 2.634(5), 2.58(1), 2.702(6), and 2.667(3) Å for forms (I)—(IV), respectively. As the carboxy-group in the zwitterion is ionized, the distance for form (II) is significantly shorter than those for the other forms.

In forms (I) and (II), the molecules are linked by the intermolecular hydrogen bonds between the N(1) and O(16) atoms to form infinite chains extending along the

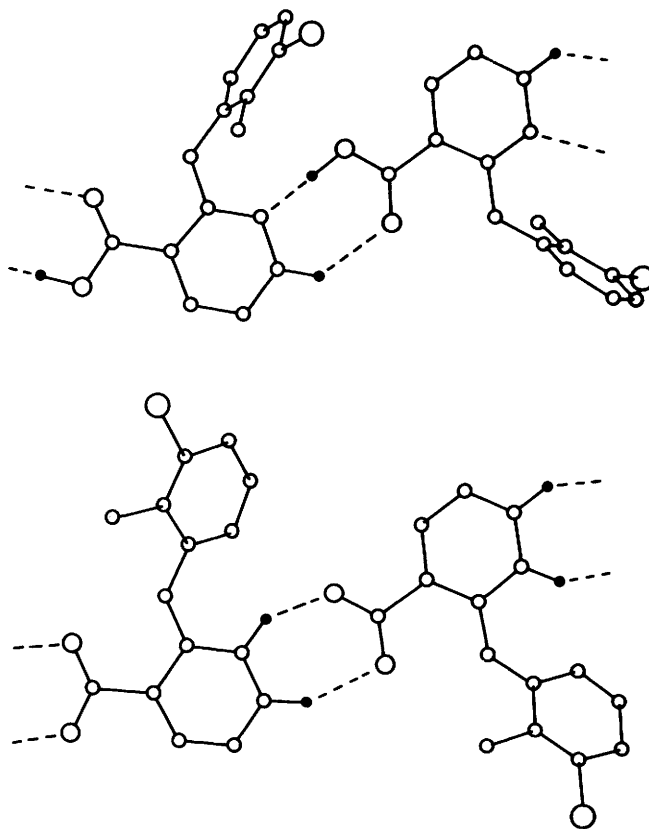


FIGURE 2 Intermolecular hydrogen bonds in forms (I) (upper) and (II) (lower)

hydrogen bond $\text{>CH} \cdots \text{O}$ was suggested by these values, but could not be confirmed by i.r. spectroscopic evidence as the CH stretching bands could not be identified.

The two molecules related by an inversion centre in forms (III) and (IV) form the dimer molecule linked by the hydrogen bonds between the carboxy-groups. The distances of O(16) ··· O(17) are respectively 2.649(6) and 2.694(3) Å for forms (III) and (IV).

The intra- and inter-molecular hydrogen bonds in the forms proposed by the present i.r. spectral study have consequently been confirmed by the X-ray study.

TABLE 4

Atomic co-ordinates ($\times 10^4$, and $\times 10^3$ for hydrogen) and equivalent isotropic temperature factors with estimated standard deviations in parentheses

Form (I)	x	y	z	$B_{eq}/\text{Å}^2$
N(1)	5 110(3)	4 196(2)	2 101(2)	3.44(7)
C(2)	5 460(4)	5 068(2)	2 555(3)	3.28(9)
C(3)	4 511(4)	5 870(2)	2 025(3)	2.96(9)
C(4)	3 212(4)	5 734(2)	1 020(3)	3.76(9)
C(5)	2 888(5)	4 847(3)	554(3)	4.35(10)
C(6)	3 866(5)	4 109(2)	1 110(3)	3.96(10)
N(7)	6 729(4)	5 157(2)	3 544(2)	4.12(8)
C(8)	7 806(4)	4 403(2)	4 127(3)	3.44(9)
C(9)	9 140(4)	4 006(2)	3 627(3)	3.61(9)
C(10)	10 132(4)	3 281(3)	4 254(3)	4.06(10)
C(11)	9 876(5)	3 001(3)	5 321(3)	4.34(11)
C(12)	8 592(5)	3 426(3)	5 800(3)	5.33(12)
C(13)	7 536(5)	4 129(3)	5 197(3)	4.93(12)
C(14)	9 498(5)	4 335(3)	2 485(3)	5.67(13)
C(15)	4 860(4)	6 814(2)	2 531(3)	3.44(9)
O(16)	3 906(3)	7 489(2)	1 943(2)	4.54(7)
O(17)	5 942(3)	6 965(2)	3 425(2)	5.07(8)
Cl	11 736(2)	2 704(1)	3 665(1)	8.68(5)
H(4)	258(5)	631(3)	69(3)	3.5
H(5)	202(5)	472(3)	-12(3)	3.9
H(6)	370(5)	345(3)	78(3)	3.7
H(7)	679(5)	577(3)	389(3)	3.8
H(11)	1 047(5)	248(3)	578(3)	4.1
H(12)	845(6)	323(3)	655(4)	5.1
H(13)	654(5)	445(3)	554(3)	4.5
H(14)	880(5)	391(3)	180(4)	5.1
H'(14)	1 061(5)	429(3)	243(4)	5.1
H''(14)	913(6)	500(3)	232(4)	5.1
H(16)	427(5)	819(3)	232(3)	4.1

Form (II)	x	y	z	$B_{eq}/\text{Å}^2$
N(1)	2 483(3)	1 072(15)	6 064(7)	5.49(17)
C(2)	2 728(3)	-634(18)	5 194(8)	3.82(19)
C(3)	2 340(3)	-2 152(20)	4 437(8)	4.15(23)
C(4)	1 769(3)	-1 955(20)	4 629(7)	2.21(22)
C(5)	1 556(3)	-237(25)	5 537(8)	2.93(25)
C(6)	1 927(3)	1 268(20)	6 208(8)	1.87(24)
N(7)	3 277(2)	-817(17)	5 062(8)	2.36(18)
C(8)	3 729(3)	510(21)	5 667(8)	2.35(23)
C(9)	4 196(3)	1 758(21)	5 081(9)	3.40(23)
C(10)	4 640(3)	3 050(23)	5 656(9)	2.68(26)
C(11)	4 650(4)	2 998(26)	6 797(9)	2.70(31)
C(12)	4 179(4)	1 690(27)	7 335(10)	2.98(28)
C(13)	3 728(4)	457(28)	6 828(8)	3.43(28)
C(14)	4 210(4)	1 694(28)	3 829(9)	4.25(32)
C(15)	2 556(3)	-3 960(21)	3 396(8)	4.19(25)
O(16)	2 180(2)	-5 079(19)	2 818(6)	3.69(17)
O(17)	3 074(2)	-4 023(17)	3 267(6)	4.39(19)
Cl	5 226(1)	4 699(7)	5 006	2.56(8)
H(1)	280	288	648	2.2
H(4)	155	-290	400	1.6
H(5)	114	20	570	2.4
H(6)	173	220	692	2.4
H(7)	338	-200	440	2.5
H(11)	500	380	720	3.7
H(12)	419	170	810	4.1
H(13)	341	-70	720	3.1
H(14)	455	0	350	3.7
H'(14)	455	320	350	3.7
H''(14)	392	130	340	3.7

TABLE 4 (continued)

Form (III)	x	y	z	$B_{eq}/\text{Å}^2$
N(1)	1 256(3)	3 008(12)	5 241(4)	4.22(15)
C(2)	2 169(4)	4 494(14)	5 449(5)	2.81(16)
C(3)	2 675(4)	6 013(14)	4 518(5)	3.31(16)
C(4)	2 182(4)	5 871(15)	3 362(5)	1.48(19)
C(5)	1 234(4)	4 365(15)	3 164(5)	2.40(19)
C(6)	808(4)	2 917(16)	4 120(5)	0.99(19)
N(7)	2 609(3)	4 556(12)	6 610(4)	1.40(15)
C(8)	2 279(4)	3 344(14)	7 688(5)	1.50(17)
C(9)	2 995(4)	2 803(14)	8 620(5)	2.50(17)
C(10)	2 658(4)	1 712(14)	9 691(5)	1.89(18)
C(11)	1 678(4)	1 077(17)	9 868(6)	1.88(21)
C(12)	1 004(4)	1 711(18)	8 946(6)	2.11(21)
C(13)	1 290(4)	2 829(16)	7 851(5)	2.76(20)
C(14)	4 062(4)	3 525(16)	8 442(5)	3.18(20)
C(15)	3 687(4)	7 660(15)	4 725(5)	3.02(17)
O(16)	4 020(3)	9 066(11)	3 777(3)	2.79(13)
O(17)	4 193(3)	7 723(11)	5 703(3)	3.61(13)
Cl	3 488(1)	949(5)	10 894(1)	2.01(5)
H(4)	258(4)	703(14)	274(5)	3.2
H(5)	93(4)	432(14)	236(5)	3.4
H(6)	9(4)	210(14)	407(5)	3.4
H(7)	320(4)	525(14)	664(5)	2.9
H(11)	144(4)	35(15)	1 060(5)	4.0
H(12)	33(4)	173(15)	907(5)	4.2
H(13)	78(4)	341(14)	718(5)	3.7
H(14)	434(4)	596(15)	858(5)	3.7
H'(14)	428(4)	222(14)	768(5)	3.7
H''(14)	451(4)	287(15)	919(5)	3.7
H(16)	464(4)	1 031(15)	411(5)	3.9

Form (IV)	x	y	z	$B_{eq}/\text{Å}^2$
N(1)	6 135(2)	1 534(2)	3 459(2)	8.35(4)
C(2)	4 853(2)	2 241(2)	4 094(2)	8.83(5)
C(3)	3 118(3)	2 695(2)	3 425(2)	8.72(5)
C(4)	2 784(3)	2 356(3)	2 100(2)	6.02(6)
C(5)	4 120(3)	1 616(3)	1 466(2)	6.47(6)
C(6)	5 751(3)	1 264(3)	2 191(2)	4.36(6)
N(7)	5 212(2)	2 531(2)	5 390(2)	4.27(4)
C(8)	6 760(2)	2 258(2)	6 287(2)	6.95(5)
C(9)	6 611(2)	2 771(3)	7 582(2)	6.66(5)
C(10)	8 139(3)	2 584(3)	8 494(2)	6.61(6)
C(11)	9 747(3)	1 876(3)	8 187(2)	5.05(6)
C(12)	9 834(3)	1 373(3)	6 927(2)	4.42(6)
C(13)	8 363(3)	1 553(3)	5 969(2)	4.30(6)
C(14)	4 885(3)	3 500(3)	7 938(2)	7.54(6)
C(15)	1 715(3)	3 570(3)	4 092(2)	9.37(5)
O(16)	181(2)	3 830(2)	3 344(2)	6.90(4)
O(17)	1 949(2)	4 047(2)	5 258(1)	8.36(4)
Cl	8 102(1)	3 227(1)	10 115(1)	5.32(2)
H(4)	168(4)	270(3)	166(3)	3.4
H(5)	389(4)	151(3)	59(3)	3.6
H(6)	677(4)	76(3)	179(3)	3.5
H(7)	428(3)	299(3)	572(2)	3.0
H(11)	1 074(4)	188(3)	887(3)	3.7
H(12)	1 098(4)	82(4)	669(3)	3.9
H(13)	844(4)	129(3)	508(3)	3.2
H(14)	394(4)	260(3)	760(3)	3.7
H'(14)	448(4)	465(3)	759(3)	3.7
H''(14)	493(4)	362(3)	875(3)	3.7
H(16)	-67(4)	453(3)	379(3)	3.6

Thermal differential analysis revealed that the crystal in form (I) is not transformed into any other form during the heating process to the m.p. 242 °C. Forms (II)—(IV), however, are transformed into a fifth form at the transition points of 159, 156, and 144 °C, respectively and melt at the same temperature as form (I). Since the fifth form gives the same i.r. spectrum as that of form (I) at room temperature, it is assumed to be identical to form (I).

Correlation between I.r. Spectral and Structural Data.—For the AH ··· B intermolecular hydrogen bond, the

wavenumber (ν_{AH}) of the AH stretching band decreases as the hydrogen bond distance ($R_{\text{A}\cdots\text{B}}$) is shortened. The correlations of ν_{AH} versus $R_{\text{A}\cdots\text{B}}$ have been proposed to hold theoretically and experimentally for the $\text{NH}\cdots\text{O}$, $\text{OH}\cdots\text{O}$, and $\text{OH}\cdots\text{N}$ systems.^{5,6,12}

The known relationships can be applied to the $\text{N}(1)\cdots\text{O}(16)$ in form (II) (ν_{NH} 2 712 cm^{-1} ; $R_{\text{N}\cdots\text{O}}$ 2.75 Å) and the $\text{O}(16)\cdots\text{O}(17)$ in forms (III) (ν_{OH} 2 940 cm^{-1} ; $R_{\text{O}\cdots\text{O}}$ 2.649 Å) and (IV) (ν_{OH} 3 050 cm^{-1} ; $R_{\text{O}\cdots\text{O}}$ 2.694 Å). However, the datum point of ν_{OH} versus $R_{\text{O}\cdots\text{O}}$ for $\text{O}(16)\cdots\text{N}(1)$ in form (I) (ν_{OH} 2 458 cm^{-1} ; $R_{\text{O}\cdots\text{N}}$ 2.710 Å) deviates largely from the curve^{12a} previously derived. The value of ν_{OH} on the curve corresponding to $R_{\text{O}\cdots\text{N}}$ of 2.710 Å is *ca.* 3 000 cm^{-1} .

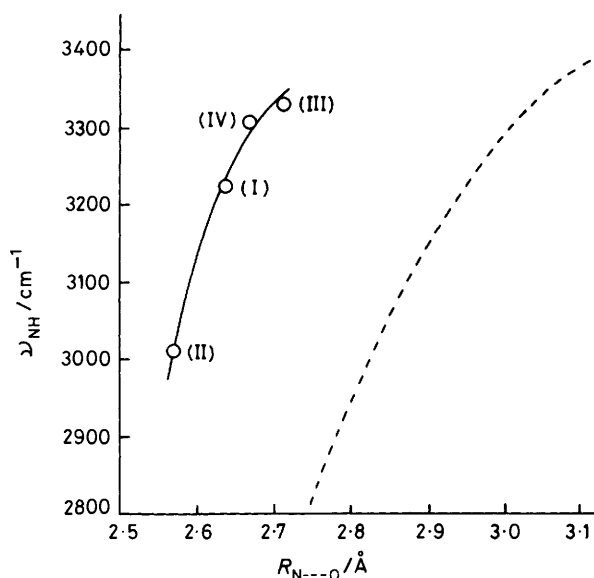


FIGURE 3 Correlation between ν_{NH} and $R_{\text{N}\cdots\text{O}}$ for intramolecular hydrogen bond system $\text{NH}\cdots\text{O}$ in forms (I)–(IV). Intermolecular hydrogen bond: — — —

The relationship of ν_{NH} versus $R_{\text{N}\cdots\text{O}}$ for the intramolecular hydrogen bonds $\text{NH}\cdots\text{O}$ formed in crystals has not been presented. The curve drawn for the intramolecular hydrogen bonds $\text{N}(7)\cdots\text{O}(17)$ in forms (I)–(IV) is shown in Figure 3, and compared with that proposed for the intermolecular hydrogen bonds. For the values of $R_{\text{N}\cdots\text{O}}$ corresponding to a fixed value of ν_{NH} , $R_{\text{N}\cdots\text{O}}$ on the former curve is shorter by 0.2–0.3 Å than that on the latter one.

Formation of the hydrogen bond $\text{AH}\cdots\text{B}$, as a rule, is accompanied by intensification of the AH stretching band. This criterion seems not to apply to the intramolecular hydrogen bonds $\text{N}(7)\cdots\text{O}(17)$, because the NH stretching bands in the spectra of all the forms are still weak. This may result from a large delocalization effect of the NH bond electrons through the hydrogen bond system.¹³

Correlation between U.v. Spectral and Structural Data.—U.v. spectral data are shown in Table 5. The band at 350 nm in the spectrum of CHCl_3 solution was assigned to the $\pi\text{--}\pi^*$ electronic transition band between the two

TABLE 5
U.v. spectral data of 2(2M3CA)NA

Form	$\lambda_{\text{max.}} / \text{nm}$	
	(I)	270
(II)	282	354
(III)	291	374
(IV)	288	379
	292 ^a	350 ^a
	(16 200) ^b	(5 290) ^b

^a In CHCl_3 . ^b The values in parentheses are $\epsilon_{\text{max.}}$ ($\text{cm}^{-1} \text{mol}^{-1} \text{dm}^3$) in CHCl_3 .

chromophores because of its strong intensity and appearance at the longer wavelength. The corresponding bands in crystalline states are shifted to longer wavelengths in the order of forms (I)–(IV). Such a red shift seemed to be accompanied by a decrease in the twist angle (θ) of the benzene ring about the $\text{N}(7)\text{--C}(8)$ bond as described above. The relation between the wavelength and the value of $\cos^2 \theta$ was found to be linear (r 0.99) as seen in Figure 4. The θ value of the molecule

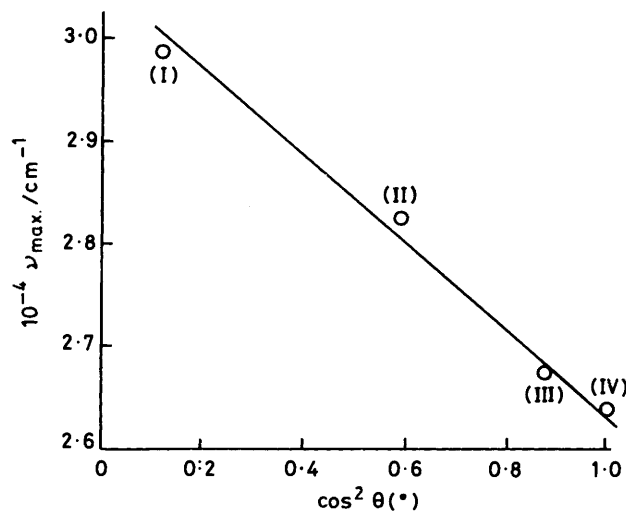


FIGURE 4 Correlation between $\nu_{\text{max.}}$ and $\cos^2 \theta$ in forms (I)–(IV)

in CHCl_3 solution was estimated to be *ca.* 48°, using this relationship.

The HMO method showed by an approximation of the second-order perturbation, that the energy difference between ground and excited states in a molecule consisting of two conjugated moieties changes in proportion to the square of the resonance integral.¹⁴ The value of the resonance integral is proportional approximately to the value of the overlap integral and, accordingly, to $\cos \theta$. This may result in the linear relationship between the wavelength and $\cos^2 \theta$ observed in the four forms. The variation in crystal colours as shown in Table 1, therefore, can be explained in terms of the change in the π -conjugation between the benzene and pyridine rings through the lone pair orbital of $\text{N}(7)$.

We thank Miss K. Nagano for suggesting this investigation and Drs. Y. Matsui, M. Yamakawa, and K. Ezumi,

our laboratories, for helpful discussions. Our thanks are also due to Professor T. Kubota, Gifu College of Pharmacy, for his continuing interest throughout this investigation.

[1/1732 Received, 9th November, 1981]

REFERENCES

- ¹ W. B. Wright and G. S. D. King, *Acta Crystallogr.*, 1953, **6**, 305.
- ² F. Takusagawa, K. Hirotsu, and A. Shimada, *Bull. Chem. Soc. Jpn.*, 1973, **46**, 2020, 2292, 2372, 2669.
- ³ G. A. Sim, J. M. Robertson, and T. H. Goodwin, *Acta Crystallogr.*, 1955, **8**, 157.
- ⁴ K. Nakamoto, M. Margoshes, and R. E. Rundle, *J. Am. Chem. Soc.*, 1954, **77**, 6480.
- ⁵ A. Lautié, F. Froment, and A. Novak, *Spectrosc. Lett.*, 1976, **5**, 289.
- ⁶ A. Novak, *Struct. Bonding*, 1974, **18**, 177.
- ⁷ A. Lautié and A. Novak, *Chem. Phys. Lett.*, 1980, **71**, 290.
- ⁸ P. Main, G. Germain, and M. M. Woolfson, 'MULTAN: A System of Computer Programs for the Automatic Solution of Noncentrosymmetric Crystal Structure,' University of York.
- ⁹ D. F. Grant, R. C. G. Killean, and J. L. Lawrence, *Acta Crystallogr.*, 1969, **B25**, 347.
- ¹⁰ 'International Tables for X-Ray Crystallography,' Kynoch Press, Birmingham, 1962, vol. III.
- ¹¹ T. C. Downin and J. C. Speakman, *J. Chem. Soc.*, 1954, 784.
- ¹² (a) R. Schroeder and E. R. Lippincott, *J. Phys. Chem.*, 1957, **61**, 921; (b) E. R. Lippincott and R. Schroeder, *J. Chem. Phys.*, 1955, **23**, 1099.
- ¹³ M. Takasuka and Y. Matsui, *J. Chem. Soc., Perkin Trans. 2*, 1979, 1743.
- ¹⁴ K. Fukui, K. Morokuma, T. Yonezawa, and C. Nagata, *Bull. Chem. Soc. Jpn.*, 1960, **33**, 963.